



Controlling of the single domain wall propagation in magnetic microwires by magnetostatic interaction

Paula Corte-Leon^{a,b,c,d}, Alvaro Gonzalez^{a,b,c}, Juan Maria Blanco^{b,c}, Valentina Zhukova^{a,b,c}, Mihail Ipatov^e, Julian Gonzalez^{a,c}, Arcady Zhukov^{a,b,c,f,*}

^a Department of Polymers and Advanced Materials, University of Basque Country, UPV/EHU, 20018, San Sebastian, Spain

^b Department of Applied Physics, EIG, UPV/EHU, 20018, San Sebastian, Spain

^c EHU Quantum Center, University of the Basque Country, UPV/EHU, Spain

^d Department of Materials Science & Metallurgy, University of Cambridge, 27 Charles Babbage Road, Cambridge, CB3 0FS, UK

^e Servicios Generales de Investigación (SGIker), Bilbao, Spain

^f IKERBASQUE, Basque Foundation for Science, 48011, Bilbao, Spain

ARTICLE INFO

Keywords:

Domain wall dynamics
Magnetostatic interaction
Stray field
Demagnetizing factor

ABSTRACT

Ultrafast magnetization switching through the single domain wall (DW) propagation has been reported in amorphous micrometric and submicrometric wires. However the performance of prospective devices utilizing DW propagation is determined by the degree to which DW propagation can be controlled. In this article, we propose a novel method for effectively controlling the single DW propagation in a specially designed array consisting of two magnetic microwires by the stray field from magnetically softer microwires. We have experimentally demonstrated that the DW velocity of magnetically harder Fe-rich microwire in such a linear array is affected by the stray field of magnetically softer Co-rich microwire. Additionally, the domain wall can be trapped in the Fe-rich microwire by the stray field produced by the Co-rich microwire in such a linear array. The observed effect of magnetostatic interaction depends on the position of the Co-rich microwire in such a linear array. Controllable domain wall propagation observed in such a linear array can be a useful tool for simple and more flexible ways of controllable trapping and braking of single DWs in Fe-rich microwires showing spontaneous magnetic bistability.

1. Introduction

Magnetic wires have attracted considerable attention due to their rather attractive magnetic properties, such as magnetic bistability or giant magneto-impedance (GMI) effect [1–5], potentially suitable for several prospective applications (magnetic and magnetoelastic sensors, magnetic memory and logic, electronic surveillance, etc.) [2,3,6–9].

Among different families of magnetic wires, amorphous magnetic wires produced by rapid quenching from the melt present clear advantages, such as superior magnetic softness as well as excellent mechanical properties [10–13]. Therefore, the studies of amorphous magnetic wires have become the subject of intensive research over the past 4 decades.

There are several preparation techniques allowing the fabrication of amorphous magnetic wires [5,10–12]. The so-called Taylor-Ulitovsky technique allows the preparation of magnetic wires with the most

extended diameters range (within 4 orders of magnitude): from submicrometric (0.1 μm) [14] to 100 μm diameters [15]. The fabrication method is fast (up to 100 m per minute) and low cost [16–18]. Additionally, such magnetic wires are covered with flexible and insulating glass coating and have cylindrical metallic nuclei [13,14,16–18]. Accordingly, in addition to the excellent magnetic softness and superior mechanical properties, such glass-coated microwires present enhanced corrosion resistance and biocompatibility [12,16,19]. Therefore, studies of glass coated magnetic microwires generated huge interest due to emerging prospective applications [9,19–23].

As mentioned above, amorphous magnetic wires can present magnetic bistability associated with fast magnetization switching through large and single Barkhausen jump [16,23–25]. The hysteresis loop of such magnetic wires presents perfectly rectangular shape. The origin of magnetic bistability is the remagnetization process of single domain

Peer review under responsibility of Vietnam National University, Hanoi.

* Corresponding author. Department of Polymers and Advanced Materials, University of Basque Country, UPV/EHU, 20018, San Sebastian, Spain.

E-mail address: arkadi.joukov@ehu.es (A. Zhukov).

<https://doi.org/10.1016/j.jسامd.2024.100712>

Received 12 December 2023; Received in revised form 28 February 2024; Accepted 21 March 2024

Available online 28 March 2024

2468-2179/© 2024 Vietnam National University, Hanoi. Published by Elsevier B.V. This is an open access article under the CC BY license (<http://creativecommons.org/licenses/by/4.0/>).

with axial magnetization orientation through the fast domain wall (DW) propagation [23–25]. Such peculiar feature of magnetic wires is considered among the most promising phenomena, from the viewpoint of applications [16,23–27].

Among the most promising applications involving either controllable DW propagation or perfectly rectangular hysteresis loops observed in amorphous nano- and microwires are racetrack memory, magnetic logics, magnetic and magnetoelastic sensors or electronic surveillance [6–9,23,24,27,28].

As regarding the single DW propagation, the principal advantage of amorphous wires is unusually high DW velocity, v : $v \geq 1$ km/s are commonly reported for various families of amorphous wires [23,26,27]. Such v – values can be further improved by appropriate processing of amorphous microwires, such as annealing or application of a transverse magnetic field [23,26,27].

On the other hand, the degree of control over DW propagation in ferromagnets is another issue for implementing the above-mentioned DW propagation applications [27–29]. However, only a few successful attempts involving controlled DWs injection, propagation, or pinning in amorphous microwires have been reported [30–34]. At the same time, the influence of various factors (applied stresses, annealing, applied transverse field, induced magnetic anisotropy or graded magnetic anisotropy, distribution of defects along the wire) on the DW dynamics in amorphous microwires was previously reported [27].

Accordingly, in this paper, we provide recent experimental results on the manipulation of single DW propagation in amorphous Fe-rich glass-coated microwires by magnetostatic interaction with other Co-rich glass-coated microwires.

2. Experimental

The DW dynamics was studied in as-prepared 12 cm long $\text{Fe}_{69}\text{B}_{12}\text{Si}_{14}\text{C}_5$ microwire (metallic nucleus diameter $d = 19.8 \mu\text{m}$, total diameter $D = 28.6 \mu\text{m}$) with positive magnetostriction coefficient, λ_s , (38×10^{-6}) [27] as well as in a linear array consisting of the same 12 cm long $\text{Fe}_{75}\text{B}_9\text{Si}_{12}\text{C}_4$ microwire and 1 cm long Co-rich microwire ($\text{Co}_{64.6}\text{Fe}_{5.8}\text{B}_{16.8}\text{Si}_{11}\text{Cr}_{3.4}$, $d = 80 \mu\text{m}$, $D = 92.3 \mu\text{m}$) placed near Fe-rich microwire (see Fig. 1). In all the cases, the samples have been inserted

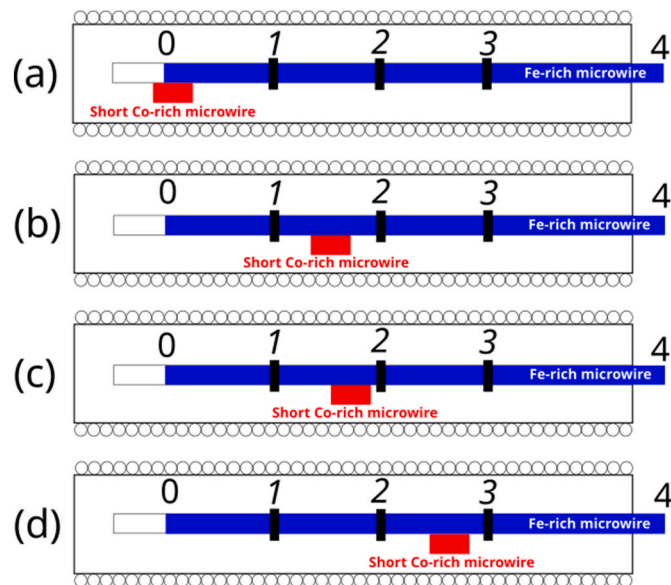


Fig. 1. The schematic sketch of the experimental set-up (1,2,3- pick-up coils, 0- sample end inside the solenoid, 4- sample end outside the solenoid) and the position of Fe-rich and Co-rich microwires with respect to magnetizing solenoid and pick-up coils during the EMF peaks measurements 0.5 cm (a); 4.5 cm (b); 5 cm (c) and 7.5 cm (d) from 0- Fe-rich sample end inside the solenoid.

inside a thin capillary. A capillary with pick-up coils was placed coaxially inside a magnetizing 140 mm long solenoid in the region with a homogeneous magnetic field. While the position of Fe-rich microwire was fixed, the measurements of DW propagation have been performed at different positions of Co-rich microwire along the Fe-rich microwire (see Fig. 1).

When we selected Co-rich microwire, we considered several factors:

- The magnetization of Co-rich microwire is lower than that of Fe-rich microwire [16,17,24].
- The macroscopic demagnetizing factor, D_{Co} , of Co-rich microwires. Although, generally the correct evaluation of D_{Co} tensor of cylinder is rather complex [35], for relatively long wire (for $\Delta = l/d \gg 1$), D_{Co} can be expressed as [36]:

$$D_{Co} = 4\pi[\ln(2\Delta) - 1]/\Delta^2 \quad (1)$$

being l is the sample length, d -metallic nucleus diameter.

Accordingly, for relatively short and thick microwire the D_{Co} -value is relatively high.

The DW propagation has been studied using modified Sixtus-Tonks-like technique based on use of three pick-up coils placed on the capillary at a distance of 27 mm from each other along the studied Fe-rich microwire [27,37]. Three pick-up coils (2 mm long and 1 mm inner diameter) have been placed inside the solenoid coaxially, surrounding the studied sample and separated by the same distance. The pick-up coils are connected to corresponding digital oscilloscope inputs. Resistors have been connected in parallel to the pick-up coils to suppress the oscillations. A homogeneous magnetic field, H , along the microwire is created by the aforementioned long (140 mm long, 10 mm in diameter) solenoid using a square waveform with a frequency of 10 Hz. A single-layer magnetizing solenoid with a reduced number of turns was used to avoid a situation where the DW could start to propagate while H is still rising. The transient time of the coil is mainly determined by the inductance, which is proportional to the square of the number of turns, N . Therefore, by reducing N , we decrease the transient time and increase the sweep rate, dH/dt . The distance between the end of the microwire and the first pick-up coil is about 40 mm, so the transient process ends when the DW reaches the first pick-up coil.

The DW velocity, v , has been evaluated from the time difference, Δt , in the electromotive force, EMF , peaks induced by the travelling DW in the pick-up coils, separated by the distance, l , as [27,37]:

$$v = \frac{l}{\Delta t} \quad (2)$$

Such setup has been previously successfully used for studies of the DW propagation in magnetic microwires [27,28].

Similarly to previous studies, one end of Fe-rich microwire is placed outside the magnetizing solenoid to ensure the DW propagation from the opposite wire end [27,28].

Both samples were prepared by the Taylor-Ulitovsky method, described in details elsewhere [16–18].

The fluxmetric method, developed for precision measurements of magnetically soft microwires at room temperature [38], has been used to measure the axial hysteresis loops of the studied microwires, as well as of the microwires array. For better comparison of microwires with different chemical compositions (and hence different saturation magnetization) and diameters we use the normalized magnetization M/M_0 versus magnetic field H , being M - the magnetic moment at a given magnetic field and M_0 - the magnetic moment of the sample at the maximum magnetic field amplitude H_{max} .

As expected from previous knowledge on magnetic properties of glass-coated microwires Fe-rich microwire with $\lambda_s > 0$ presents perfectly rectangular axial hysteresis loops (see Fig. 2a), while inclined axial hysteresis loop with much lower coercivity, H_c , ($H_c \approx 15$ A/m) is observed in Co-rich microwire with vanishing λ_s (see Fig. 2b). Such

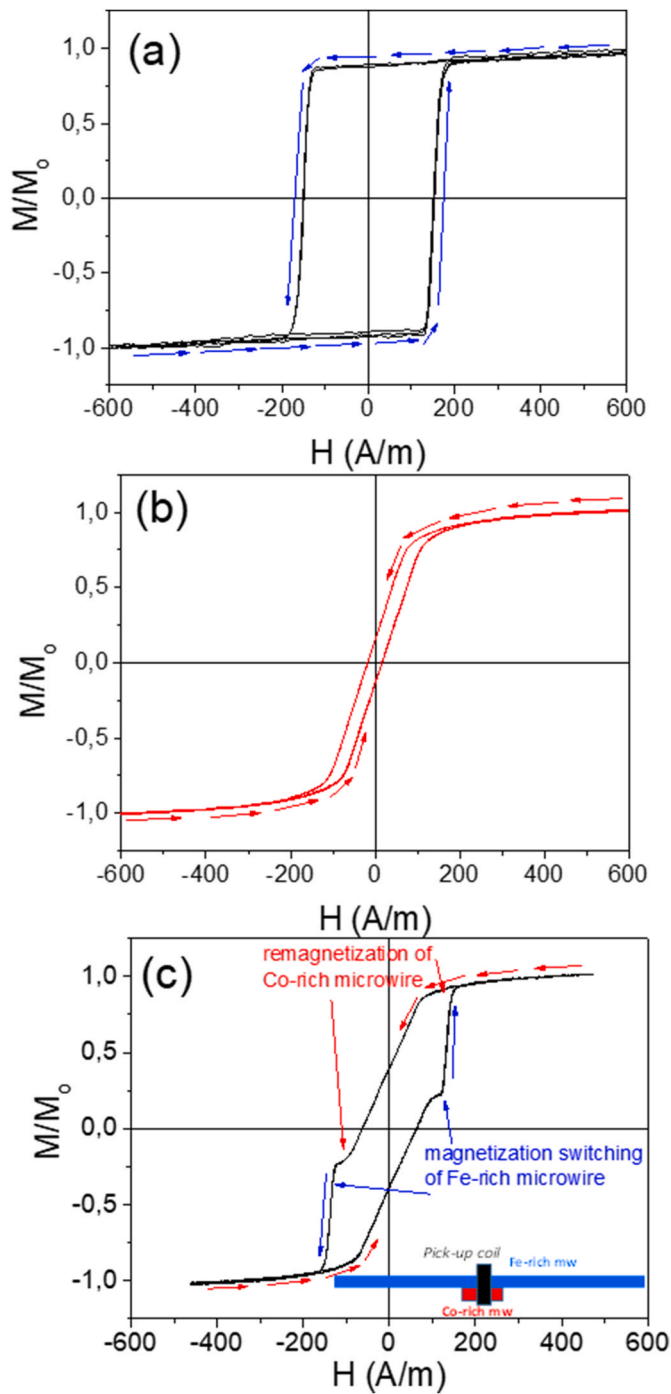


Fig. 2. Hysteresis loops of studied Fe-rich (a) and Co-rich (b) samples and linear array consisting of Fe-rich and Co-rich microwires (c).

character of axial hysteresis loops is commonly explained by the domain structure of studied microwires: the domain structure of magnetic microwires is commonly described as consisting of a single axially magnetized domain, surrounded by outer domain shell. The core-shell domain structure is commonly reported both experimentally (using Magneto-optical Kerr effect, MOKE, or magneto-optical indicator films, MOIF methods) [39–43] and theoretically [44] in magnetic wires. Bamboo-like domain structure is typically observed in the outer shell of Co-rich magnetic wires with vanishing magnetostriction [39–41]. While, radially oriented domains are reported in the outer shell for Fe-rich microwires [39,42–44]. The schematic picture of domain structures of Fe-rich and Co-rich microwires is provided in Fig. 3.

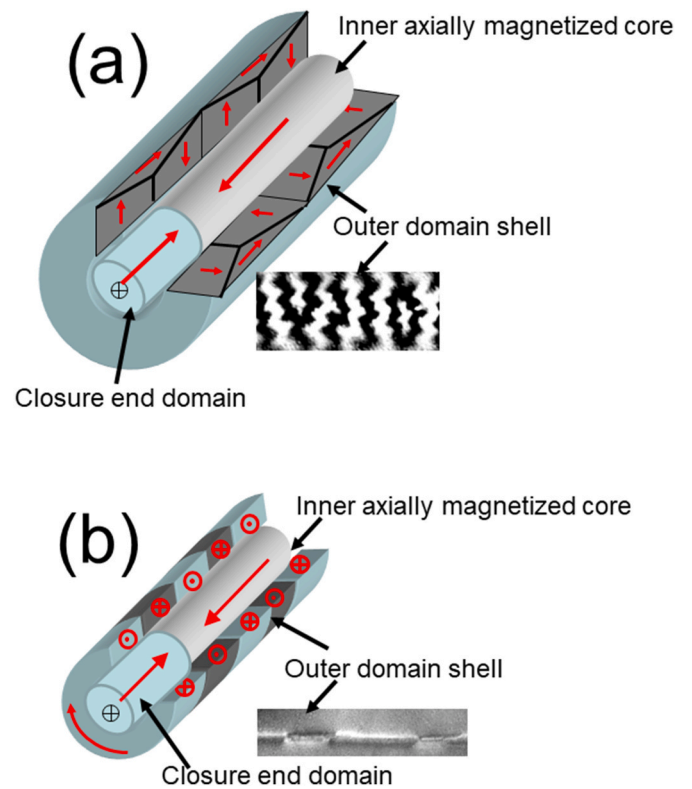


Fig. 3. Schematic pictures of domain structure of Fe-rich (a) and Co-rich (b) microwires.

The remagnetization process of Fe-rich microwires runs by the depinning of single DW from one of the closure end domains and subsequent DW propagation along the entire inner core [25–27,30]. Instead, the remagnetization process of Co-rich microwires usually present low coercivity and high magnetic permeability [21,38].

The axial hysteresis loops of the array consisting of one $\text{Fe}_{69}\text{B}_{12}\text{Si}_{14}\text{C}_5$ and one $\text{Co}_{64.6}\text{Fe}_{5.8}\text{B}_{16.8}\text{Si}_{11}\text{Cr}_{3.4}$ microwires is shown in Fig. 2c. The unusual hysteresis loop of such linear array has been previously explained as the superposition of those of Fe-rich and Co-rich microwires with rather different remagnetization processes [45]. Briefly, from Fig. 2b we can see that the magnetization of Co-rich microwire essentially depends on applied magnetic field in low magnetic field amplitude, H_0 , region. Indeed, when the magnetic field changes from $H = -600$ A/m to $H = +600$ A/m the magnetization of Co-rich microwire starts to change from about $H = -200$ A/m (slow and reversible change) followed by more substantial change from $H \geq -120$ A/m (see Fig. 2b). The coercivity, H_c , of Fe-rich microwire is about 130 A/m (see Fig. 2a). When magnetic field changes from -130 A/m to 130 A/m, the M/M_0 of Co-rich changes from $M/M_0 \approx -0.85$ to $M/M_0 \approx +0.85$. At the same time, the magnetization of the magnetically bistable Fe-rich microwire remains almost the same (about $M/M_0 \approx -0.9$) up to $H \pm 130$ A/m. At this H -value Co-rich microwire is already magnetized in the opposite direction ($M/M_0 \approx +0.85$). Accordingly, the unusual hysteresis loop of the array consisting of Fe and Co-rich microwires (see Fig. 2c) must be explained as the superposition of magnetization processes of magnetically bistable Fe-rich microwire and magnetically soft Co-rich microwire.

We assume that at this magnetic field region the domain wall tears off from one end of the Fe-based microwire but does not have time to propagate through the whole wire because of the effect of stray field coming from Co-rich microwire. Further decreasing of H_0 below switching field of individual Fe-based sample leads to the disappearance of the influence Fe-based microwire and we observe the hysteresis loops

typical for Co-based microwire.

3. Results and discussion

As expected from the perfectly rectangular hysteresis loop of studied $\text{Fe}_{69}\text{B}_{12}\text{Si}_{14}\text{C}_5$ microwire and similarly to the previously reported experimental results on the DW dynamics in Fe-rich microwires, a linear $v(H)$ dependence is observed in studied $\text{Fe}_{69}\text{B}_{12}\text{Si}_{14}\text{C}_5$ sample (see Fig. 4a). Such DW dynamics is characterized by a sequence of the EMF signals, ε , induced in the pick-up coils by the travelling DW, as reported elsewhere [34,46,47]. It is essential to note that in the $v(H)$ dependence show in Fig. 4, the H -values are represented for the magnetic field generated by the magnetizing coil.

As previously discussed [47], the EMF , ε , generated in the turn of the pick-up coil due to the change in magnetic flux is given as:

$$\varepsilon(t) = \frac{\Delta\phi}{\Delta t} \quad (3)$$

being $\Phi = BS$ is the magnetic flux, S is the area of the surface, $B = M + H$ is the magnetic induction, and M is the magnetization. Accordingly, the EMF amplitude and width is determined by $\frac{\partial M}{\partial t}$.

The $\varepsilon(t)$ dependencies observed for Fe-rich microwire with almost the same EMF -signals amplitude and width are typical for DW propagation with a uniform velocity, when a propagating DW passes sequentially through the first, second and third pick-up coils (see Fig. 4b).

As shown below, the remagnetization in the linear array consisting of 12 cm long $\text{Fe}_{69}\text{B}_{12}\text{Si}_{14}\text{C}_5$ microwire and 1 cm long $\text{Co}_{64.6}\text{Fe}_{5.8}\text{B}_{16.8}\text{Si}_{11}\text{Cr}_{3.4}$ sample is rather different. In Fig. 5 the EMF signals, ε , induced in the pick-up coils by the remagnetization process in the array consisting of 12 cm long $\text{Fe}_{69}\text{B}_{12}\text{Si}_{14}\text{C}_5$ microwire and 1 cm long $\text{Co}_{64.6}\text{Fe}_{5.8}\text{B}_{16.8}\text{Si}_{11}\text{Cr}_{3.4}$ sample as a function of position of Co-rich microwire measured at. In the case when a piece of Co-rich microwire is placed far from the position of any pick-up coil, the peaks sequence is rather similar to that of a single Fe-rich microwire (see Fig. 5a). However, the picture changes when the 1 cm long Co-rich sample moves through the 12 cm long Fe-rich microwire. Thus, approaching Co-rich sample to the position of 1-st pick-up coil, the EMF signal in the 1-st pick-up coil becomes smaller (see Fig. 5b). Then, at certain position of Co-rich microwire (in the proximity of the 2-nd pick-up coil between 1-st and 2-nd coils), only the EMF signals in the pick-up coils 2 and 3 are observed (Fig. 5c). If we move further the 1 cm long Co-microwire along the Fe-rich microwire and when the Co-rich microwire reaches the position between 2-nd and 3-rd pick-up coils, only the EMF signal in the pick-up coil 3 is observed. Such influence of Co-rich microwires on the DW dynamics in studied linear array must be attributed to the magnetostatic interaction of 12 cm long $\text{Fe}_{69}\text{B}_{12}\text{Si}_{14}\text{C}_5$ microwire and 1 cm long $\text{Co}_{64.6}\text{Fe}_{5.8}\text{B}_{16.8}\text{Si}_{11}\text{Cr}_{3.4}$ microwires. Particularly, we must assume that stray field produced by a short Co-rich microwire allows to trap DW

propagating from the wire end placed inside the magnetizing coil. However, as reported previously [30], a new DW can be injected under effect of magnetic field in the Fe-rich microwire section after the Co-rich microwire. Therefore, at some positions of Co-rich microwires, at a given H -values EMF signals can be observed only at 2-nd and or 3-rd pick-up coils.

As previously discussed [47], the ε -signal, generated by moving DW in the pick-up coil turn can be expressed as:

$$\varepsilon(t) = -\frac{2\pi Qv}{c} \frac{R^2}{(z + R^2)^{3/2}} \quad (4)$$

where c is the speed of light, R is the radius of the coil turn, $v = -dz/dt$ -DW velocity and Q -magnetic charge. The eq. (4) is obtained for the case if the characteristic DW width, δ , is small as-compared with the distance, z , between the pick-up coil turn and the DW.

The difference in EMF signals must be attributed to the change in Qv product. Accordingly, the EMF modification observed in Fig. 5b and 5c must be attributed to the different DW velocity, v , values [47].

Observed changes in $\varepsilon(t)$ dependencies must be attributed to the influence of the stray field from Co-rich microwire on DW dynamics of Fe-rich microwire.

From Fig. 2 it is important to note, that the magnetic anisotropy field, H_k , of employed $\text{Co}_{64.6}\text{Fe}_{5.8}\text{B}_{16.8}\text{Si}_{11}\text{Cr}_{3.4}$ microwire (about 110 A/m) is below the coercivity, H_c , of $\text{Fe}_{69}\text{B}_{12}\text{Si}_{14}\text{C}_5$ microwire (about 130 A/m). Therefore, when the magnetization switching of 12 cm long $\text{Fe}_{69}\text{B}_{12}\text{Si}_{14}\text{C}_5$ microwire takes place, the $\text{Co}_{64.6}\text{Fe}_{5.8}\text{B}_{16.8}\text{Si}_{11}\text{Cr}_{3.4}$ microwire is already magnetized by external field in the direction opposite to the $\text{Fe}_{69}\text{B}_{12}\text{Si}_{14}\text{C}_5$ microwire.

Such magnetized in opposite direction $\text{Co}_{64.6}\text{Fe}_{5.8}\text{B}_{16.8}\text{Si}_{11}\text{Cr}_{3.4}$ microwire produces a stray field, H_d . The H_d -value is determined by the macroscopic demagnetizing factor, D_{co} [35,48–50].

We must consider that the DW propagation in $\text{Fe}_{69}\text{B}_{12}\text{Si}_{14}\text{C}_5$ microwire takes place under the effect of a homogeneous magnetic field, H , produced by the long solenoid and the stray field, H_d , produced by $\text{Co}_{64.6}\text{Fe}_{5.8}\text{B}_{16.8}\text{Si}_{11}\text{Cr}_{3.4}$ microwire magnetized in the opposite direction (since its coercivity, $H_c \approx 15$ A/m). As discussed elsewhere, H_d can be expressed as:

$$H_d = D_{co} M \quad (5)$$

being M -magnetization of $\text{Co}_{64.6}\text{Fe}_{5.8}\text{B}_{16.8}\text{Si}_{11}\text{Cr}_{3.4}$ microwire. As mentioned above, correct evaluation of D_{co} tensor of the microwire is rather complex [35,48].

As previously experimentally shown [49–51], H_d -value and spatial distribution of magnetic microwires are affected by applied magnetic field, H , microwire length as well as by the domain structure of magnetic microwires. Thus, H_d -spatial distributions of Fe-rich and Co-rich magnetic microwires are rather different at low magnetic field [50]. Such difference has been attributed to the rather different domain structure of Fe-rich and Co-rich microwires [50]. However, the two-pole

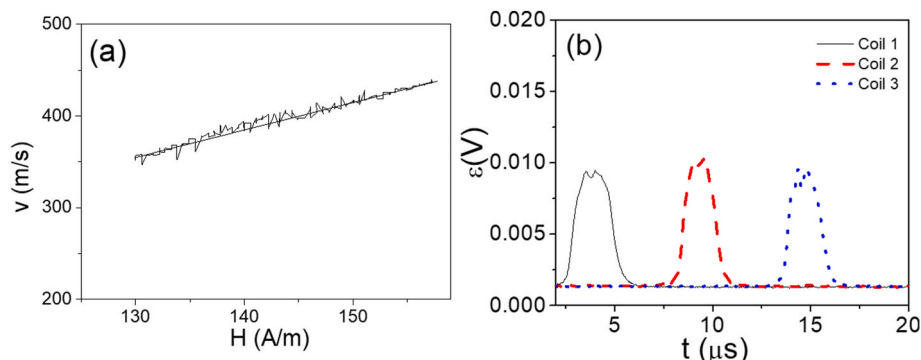


Fig. 4. $v(H)$ dependence (a) and the EMF peaks induced by the travelling DW in the pick-up coils (b) in $\text{Fe}_{69}\text{B}_{12}\text{Si}_{14}\text{C}_5$ microwire measured at $H = 135$ A/m.

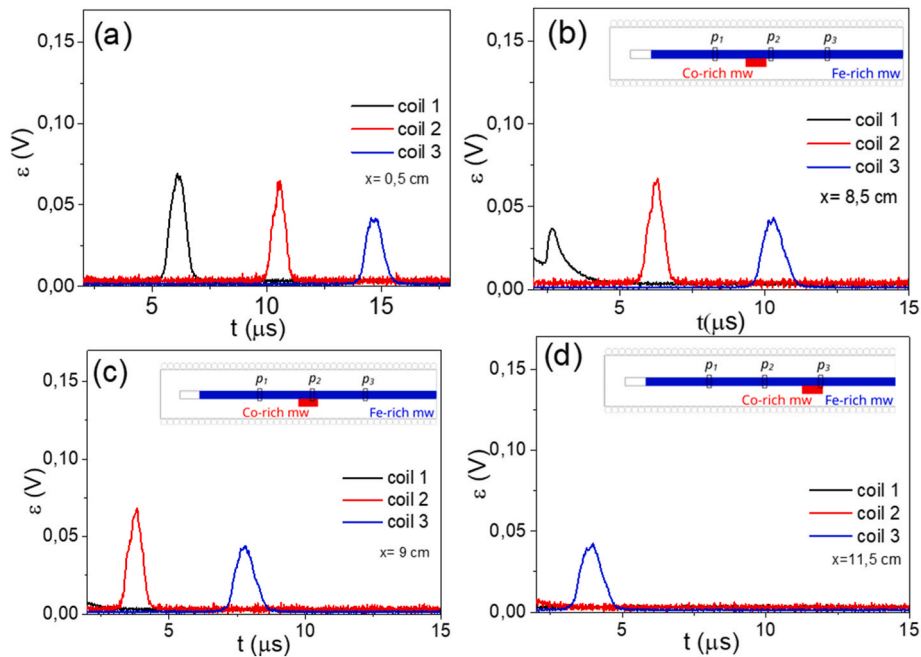


Fig. 5. The EMF peaks induced by the magnetization change in the pick-up coils in linear array consisting of 12 cm long Fe-rich and 1 cm long Co-rich microwire with different positions along the Fe-rich microwire: 0.5 cm (a); 4.5 cm (b); 5 cm (c) and 7.5 cm (d) recorded at $H = 130$ A/m.

magnetic structure has been observed at high enough external magnetic field [49]. Additionally, even at $H > H_k$, H_d -value and spatial distribution (axial and vertical components) are affected by the distance along the microwire and the distance to the microwire center [49,50]. Close to the magnetized microwire ends the magnetic field component normal to the microwire axis is experimentally observed [50,51]. The amplitude of stray magnetic fields oriented normally to the microwire axis at the wire ends reached maximum values and reduces to zero, moving further from the wire end [50,51]. On the other hand, when the magnetostatic interaction of magnetically bistable microwires was discussed, it was roughly assumed that H_d is directed against the applied magnetic field, H [45]. Accordingly, if the stray field produced by a short Co-rich microwire is opposite to the magnetic field produced by the solenoid, the DW can be braked or even pinned. However, under the effect of stray field directed transverse to the applied magnetic field, H or even with H_d component directed in the same direction as the applied magnetic field, H , new DW can be injected. Such influence of transverse magnetic field on DW injection is previously reported [52]. In this case, at a given H -values EMF signals can be observed only at 2-nd and/or 3-rd pick-up coils as observed in Fig. 5c and 5d.

In the present case, Co-rich microwire with $H_c \approx 15$ A/m is remagnetized even by low reversal magnetic field, while the DW propagation within the Fe-rich microwire takes place. The schematic sketch of the remagnetization process in a linear array consisting of long Fe-rich microwire and short Co-rich microwire is shown in Fig. 6.

The shape of travelling DW can be critical for the detailed consideration of the effect of stray field on DW dynamics. Studies of the shape

of the propagating DW in magnetic microwires is a topic of many previous papers [27,53–59]. Briefly, from the rigorous analysis of the EMF peaks induced by the propagating DW in the pick-up coils it was reported that such DW is rather extended. Thus, in contrast to nanowires where the characteristic DW width, δ_w , is of the order of the wire diameter ($\delta_w/d \sim 1-2$), in amorphous glass-coated Fe-rich microwires the EMF peak shape fits better to $\delta_w/d \sim 35-75$ [53]. Accordingly, the DW extension in studied Fe-rich microwires must be of the order of 1 mm.

Several attempts to evaluate the DW shape from the EMF peaks or from the MOKE studies have been made [54–58]. Most of the experimental data (obtained using the EMF peak shape analysis and/or magneto-optical Kerr effect, MOKE) have been interpreted considering either conical, planar, narrow tail at one end close to cylindrical at the other end and even deformed conical-like DW shapes.

It is worth noting, that the direct experimental confirmation of the DW shape is unlikely possible, since even MOKE studies can be performed only in the microwire surface, while magnetization switching in amorphous microwires takes place within the whole microwire diameter. Extremely large δ_w/d -values observed in amorphous glass-coated microwires must be attributed to rather complex DW shape.

In the present case there are the following general features that must be considered:

- The propagating DW separates two domains with the opposite magnetization inside the inner core of microwire with axially oriented magnetization.
- The DW extension in studied Fe-rich microwires is about 1 mm, being an order of magnitude lower than the length of Co-rich microwire with the opposite magnetization at the moment of the DW propagation (see Fig. 6).

From aforementioned description it looks clear that the stray field produced by shorter Co-rich microwire can affect the DW dynamics of neighboring Fe-rich microwire. Previously, a modification of DW dynamics in a linear array consisting of two magnetically bistable microwires is already reported [32]. The influence of the position of Co-rich microwire on DW dynamics in $\text{Fe}_{69}\text{B}_{12}\text{Si}_{14}\text{C}_5$ microwire is shown in

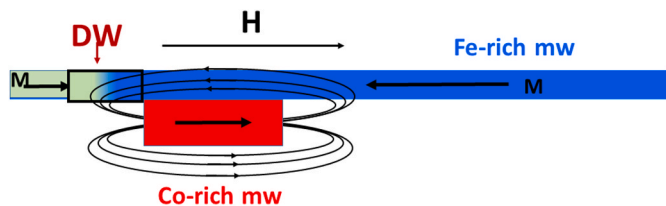


Fig. 6. Schematic sketch of the remagnetization process in a linear array consisting of long Fe-rich microwire and short Co-rich microwire.

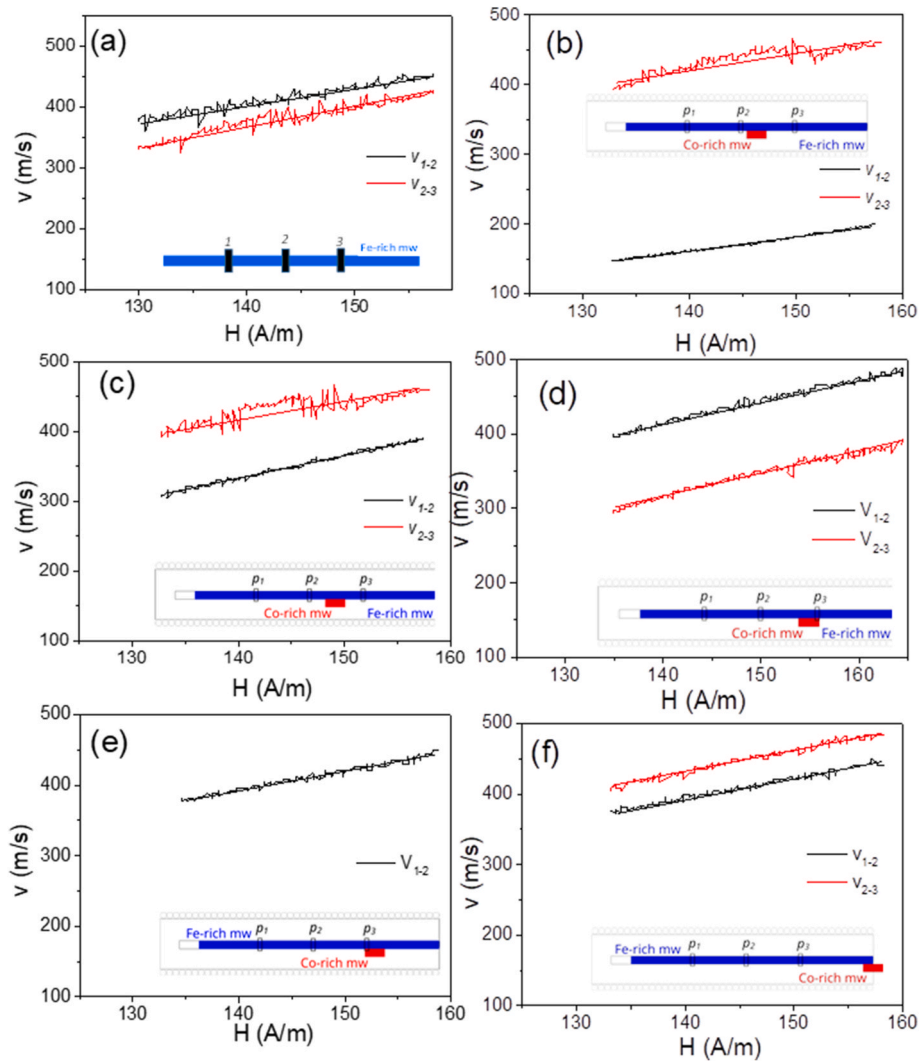


Fig. 7. $v(H)$ dependencies of single $\text{Fe}_{69}\text{B}_{12}\text{Si}_{14}\text{C}_5$ microwire (a) and linear array consisting of 12 cm long Fe-rich and 1 cm long Co-rich microwire with different positions along the Fe-rich microwire: 6 cm(b), 6.5 cm (c), 8.5 cm (d), 9.3 cm (e) and 11.5 cm (f).

Fig. 7. As shown in Fig. 7a, in the single $\text{Fe}_{69}\text{B}_{12}\text{Si}_{14}\text{C}_5$ microwire (without Co-rich microwire) the DW wall travels with almost constant velocity: DW velocities between 1-st and 2-nd and 2-nd and 3-rd pick-up coils, v_{1-2} and v_{2-3} , respectively, are almost identical. However, the DW dynamics in the presence of Co-rich microwire can be rather different. When the Co-rich microwire moves towards the pick-up coil 1, the v_{1-2} - values become substantially lower than v_{2-3} - values (see Fig. 7b). With further movement of the Co-rich microwire behind the pick-up coil 1, the v_{1-2} - values become higher (see Fig. 7c). Interesting, that while the position of Co-rich microwire is far from the coils 2 and 3 the v_{2-3} - values are almost unchanged (see Fig. 7b and c). However, moving Co-rich microwire towards pick-up coils 2 and 3 the v_{1-2} - values become higher, while the v_{2-3} - values become lower (see Fig. 7d). At certain position of Co-rich microwire along the Fe-rich microwire (when the Co-rich is moved behind pick-up coil 2 and closer to the pick-up 3) only the signals on pick-up coils 1 and 2 are observed (see Fig. 7e). At such Co-rich microwire position the v_{1-2} - values become similar to the case shown in Fig. 7 b,c, (when Co-rich microwire is far from any pick-up coils), while v_{2-3} value cannot be detected. At this Co-rich microwire position the moving DW is trapped between the pick-up coils 2 and 3. Finally, when the Co-rich microwire is placed far from the pick-up coils 1, 2, 3, the DW dynamics is still rather similar to the case of single Fe-rich microwire, (see Fig. 7f).

As mentioned above, the DW velocity is a function of the magnetic

field. The magnetic field acting on the DW is influenced by the superposition of the magnetic field created by the magnetizing solenoid and the stray field from the Co-rich microwire magnetized in the opposite direction. This is the reason why the DW dynamics is affected by the position of the Co-rich microwire: when the Co-rich microwire is located close to the travelling DW, the stray field generated by the Co-rich microwire affects the DW dynamics. Since the direction of the stray field roughly has the opposite direction to the magnetic field generated by the solenoid, a stronger external magnetic field is required for DW propagation. Therefore, the DW velocity and magnetic field at which DW dynamics is observed are affected by the position of the Co-rich microwire.

Thus, in the linear array consisting of 12 cm long $\text{Fe}_{69}\text{B}_{12}\text{Si}_{14}\text{C}_5$ microwire and 1 cm long $\text{Co}_{64.6}\text{Fe}_{5.8}\text{B}_{16.8}\text{Si}_{11}\text{Cr}_{3.4}$ microwire the v_{1-2} - and v_{2-3} - values are tunable by the position of the Co-rich microwire. In this way, travelling DW can be braked and even trapped by the magnetostatic interaction with magnetically softer short microwire in the linear array.

Such difference must be attributed to the superposition of the applied magnetic field and stray field from the 1 cm long $\text{Co}_{64.6}\text{Fe}_{5.8}\text{B}_{16.8}\text{Si}_{11}\text{Cr}_{3.4}$ microwire.

As discussed elsewhere [35,36,48,49], the stray field of a magnetic material is determined by the shape of the sample as well as by its magnetization. Accordingly, the magnetostatic interaction in the linear

array must be affected by the length, composition and diameter of magnetically softer microwires. Consequently, above described experimental results can be a useful tool for simple, and more flexible way of controllable trapping and braking of single DWs in Fe-rich microwires showing spontaneous magnetic bistability.

As discussed above, clear advantage of amorphous microwires is ultrafast DW propagation with DW velocities up to several km/s [26,27,31].

The magnetic logic elements operation (AND, NOT, OR) is determined by the degree of DW control propagation monitoring, i.e., their controllable injection, propagation, trapping or interaction. Previously, was reported that single DW propagation can be effectively pinned either by local magnetic field or by creation of artificial defects [60–62].

The stray field produced by Co-rich microwire magnetized in the opposite direction depends on its length and/or diameter. As discussed above, the magnetic field acting on travelling DW is determined by the superposition of external magnetic field and stray field produced by Co-rich microwire magnetized in the opposite direction. Accordingly, there are several parameters, such as the length and diameter of the Co-rich soft magnetic microwire or the magnitude of the external magnetic field, that can either trap or decelerate the DW travelling along the Fe-rich long microwire in determined places (see scheme in Fig. 8).

Although the experimental results provided in Figs. 4 and 6 are obtained when the length of Fe-rich microwire is about 12 cm, the magnetic bistability in Fe-rich microwire with diameter about 10 μm can be observed for the microwire of about 2 mm [36]. Therefore, the size of such magnetic logic shown in Fig. 8 can be much smaller.

It must be noted, that switching of the local magnetization of a Co microwire was previously reported through the internal stray field originated by a ferromagnetic gate electrode [63]. The similarity of observed by us effect of stray field on the DW propagation in linear microwires array and the effect of the stray field of a ferromagnetic gate on the local domain reversal lies in the controllability of the magnetic state. However, the fundamental difference between these two cases is that the DW propagation due to the stray field created by the ferromagnetic gate electrode was not achieved, while in the present case a significant change in the DW dynamics (braking and even trapping of the travelling DW) is demonstrated. Additionally, the effect of the dipolar stray fields from nearest neighbor nanowires on a ground state configuration consisting of alternating up and down magnetization in adjacent wires was observed in [Co/Pd]₁₅ and L1₀-FePt nanowire arrays [64]. In the latter case the influence of dipolar stray field on the magnetization reversal process was observed at magnetic field above 100 kA/m, i.e., 4 orders of magnitude higher H -values.

4. Conclusion

We report on the effect of magnetostatic interaction in the linear array consisting of Fe-rich magnetically bistable microwire and Co-rich microwire with soft magnetic properties. Both the hysteresis loop and the DW dynamics in such linear array are remarkably affected by the presence and position of short Co-rich microwire. The travelling DW can be either trapped or braked by the short Co-rich microwires. The origin of such magnetostatic interaction is discussed considering the superposition of the external magnetic field and the stray field produced by short Co-rich microwire already magnetized by the external field in the moment of DW propagation in the Fe-rich microwire. Such magnetostatic interaction can be a useful tool for simple, and more flexible way of controllable trapping and braking of single DWs in Fe-rich microwires showing spontaneous magnetic bistability.

Data availability

The raw/processed data required to reproduce these findings cannot be shared at this time as the data also forms part of an ongoing study.

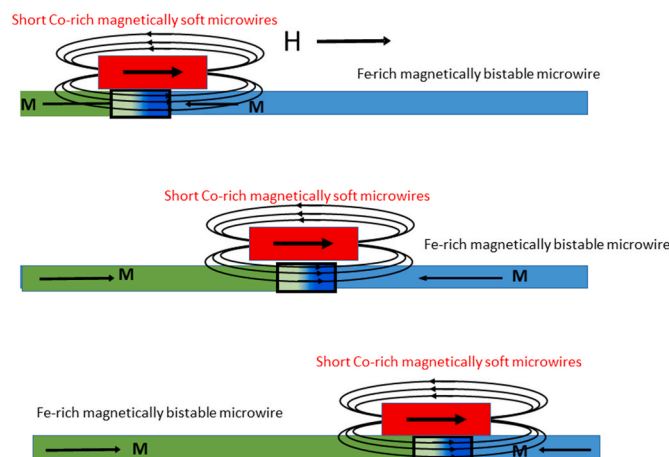


Fig. 8. Schematic picture of the engineering of DW propagation based on magnetostatic interaction in the system of linear arrays of two microwires.

Declaration of competing interest

The authors of the manuscript “Controlling of the single domain wall propagation in magnetic microwires by magnetostatic interaction” by Paula Corte-Leon, Alvaro Gonzalez, Juan Maria Blanco, Valentina Zhukova, Mihail Ipatov, Julian Gonzalez and Arcady Zhukov declare no competing financial or/and non-financial interests.

Acknowledgements

This work was supported by EU (Horizon Europe) under “INFINITE” (HORIZON-CL5-2021-D5-01-06) and “Harmony” (HORIZON-CL4-2023-RESILIENCE-01) projects, by the Spanish MICIN, under PID2022-141373NB-I00 project and by the Government of the Basque Country under Elkartek (MOSINCO) project and under the scheme of “Ayuda a Grupos Consolidados” (ref. IT1670-22). The authors thank for technical and human support provided by SGiker of UPV/EHU (Medidas Magnéticas Gipuzkoa) and European funding (ERDF and ESF). The authors wish to acknowledge useful discussions with Prof. A. Fert.

References

- [1] D.C. Jiles, Recent advances and future directions in magnetic materials, *Acta Mater.* 51 (2003) 5907–5939.
- [2] M. Knobel, M. Vazquez, L. Kraus, Giant Magnetoimpedance, *Handbook of Magnetic Materials*, vol. 15, E. Bruck, 2003, pp. 497–563.
- [3] A. Zhukov, M. Ipatov, V. Zhukova, in: K.H.J. Buschow (Ed.), *Advances in Giant Magnetoimpedance of Materials*, Handbook of Magnetic Materials, vol. 24, 2015, pp. 139–236, ch.2.
- [4] L.V. Panina, K. Mohri, Magneto-impedance effect in amorphous wires, *Appl. Phys. Lett.* 65 (1994) 1189–1191.
- [5] K. Mohri, T. Uchiyama, L.P. Shen, C.M. Cai, L.V. Panina, Amorphous wire and CMOS IC-based sensitive micro-magnetic sensors (MI sensor and SI sensor) for intelligent measurements and controls, *J. Magn. Magn. Mater.* 249 (2002) 351–356.
- [6] S.S.P. Parkin, M. Hayashi, L. Thomas, Magnetic domain-wall racetrack memory, *Science* 320 (2008) 190.
- [7] G.S.D. Beach, C. Nistor, C. Knutson, M. Tsoi, J.L. Erskine, Dynamics of field-driven domain-wall propagation in ferromagnetic nanowires, *Nat. Mater.* 4 (2005) 741–744, <https://doi.org/10.1038/nmat1477>.
- [8] D.A. Allwood, G. Xiong, C.C. Faulkner, D. Atkinson, D. Petit, R.P. Cowburn, Magnetic domain-wall logic, *Science* 309 (2005) 1688.
- [9] V. Zhukova, P. Corte-Leon, J.M. Blanco, M. Ipatov, J. Gonzalez, A. Zhukov, Electronic surveillance and security applications of magnetic microwires, *Chemosensors* 9 (2021) 100, <https://doi.org/10.3390/chemosensors9050100>.
- [10] M. Hagiwara, A. Inoue, T. Masumoto, Mechanical properties of Fe–Si–B amorphous wires produced by in-rotating-water spinning method, *Metall. Trans. A* 13A (1982) 373–382.
- [11] P. Rudkowski, G. Rudkowska, J.O. Strom-Olsen, The fabrication of fine metallic fibers by continuous melt extraction and their magnetic and mechanical properties, *Mater. Sci. Eng., A* 133 (1991) 158–161.
- [12] T. Goto, M. Nagano, N. Wehara, Mechanical properties of amorphous Fe₉₀P₁₆C₃B₁ filament produced by glass-coated melt spinning, *Trans. JIM* 18 (1977) 759–764.

- [13] V. Zhukova, A.F. Coboño, A. Zhukov, A.R. de Arellano Lopez, S. López-Pombero, J. M. Blanco, V. Larin, J. Gonzalez, Correlation between magnetic and mechanical properties of deuterified glass-coated $\text{Fe}_{71.8}\text{Cu}_1\text{Nb}_{3.1}\text{Si}_{1.5}\text{B}_{9.1}$ microwires, *J. Magn. Magn Mater.* 249 (P1-II) (2002) 79–84.
- [14] H. Chiriac, S. Corodeanu, M. Lostun, G. Ababei, T.-A. Óvári, Rapidly solidified amorphous nanowires, *J. Appl. Phys.* 107 (2010) 09A301.
- [15] P. Corte-Leon, V. Zhukova, M. Ipatov, J.M. Blanco, J. González, M. Churyukanova, S. Taskaev, A. Zhukov, The effect of annealing on magnetic properties of “Thick” microwires, *J. Alloys Compd.* 831 (2020) 150992, <https://doi.org/10.1016/j.jallcom.2019.06.094>.
- [16] A. Zhukov, P. Corte-Leon, L. Gonzalez-Legarreta, M. Ipatov, J.M. Blanco, A. Gonzalez, V. Zhukova, Advanced functional magnetic microwires for technological applications, *J. Phys. D Appl. Phys.* 55 (2022) 253003, <https://doi.org/10.1088/1361-6463/ac4fd7>.
- [17] H. Chiriac, T.A. Óvári, Amorphous glass-covered magnetic wires: preparation, properties, applications, *Prog. Mater. Sci.* 40 (5) (1996) 333–407.
- [18] S.A. Baranov, V.S. Larin, A.V. Torcunov, Technology, preparation and properties of the cast glass-coated magnetic microwires, *Crystals* 7 (2017) 136, <https://doi.org/10.3390/cryst7060136>.
- [19] D. Kozejova, L. Fecova, P. Klein, R. Sabol, R. Hudak, L. Sulla, D. Mudronova, J. Galik, R. Varga, Biomedical applications of glass-coated microwires, *J. Magn. Magn Mater.* 470 (2019) 2–5.
- [20] A. Zhukov, A.F. Coboño, J. Gonzalez, J.M. Blanco, P. Aragonese, L. Dominguez, Magnetoelastic sensor of level of the liquid based on magnetoelastic properties of Co-rich microwires, *Sensor Actuat. A Phys* 81 (1–3) (2000) 129–133.
- [21] L. Panina, A. Dzhumazoda, M. Nematov, J. Alam, A. Trukhanov, N. Yudanov, A. Morchenko, V. Rodionova, A. Zhukov, Soft magnetic amorphous microwires for stress and temperature sensory applications, *Sensors* 19 (2019) 5089, <https://doi.org/10.3390/s19235089>.
- [22] Y. Honkura, S. Honkura, The development of ASIC type GSR sensor driven by GHz pulse current, *Sensors* 20 (2020) 1023, <https://doi.org/10.3390/s20041023>.
- [23] V. Zhukova, J.M. Blanco, M. Ipatov, A. Zhukov, Effect of transverse magnetic field on domain wall propagation in magnetically bistable glass-coated amorphous microwires, *J. Appl. Phys.* 106 (2009) 113914.
- [24] K. Mohri, F.B. Humphrey, K. Kawashima, K. Kimura, M. Muzutani, Large barkhausen and matteucci effects in FeCoSiB, FeCrSiB, and FeNiSiB amorphous wires, *IEEE Trans. Magn.* 26 (1990), 1789–1781.
- [25] M. Vázquez, D.-X. Chen, The magnetization reversal process in amorphous wires, *IEEE Trans. Magn.* 31 (1995) 1229–1239.
- [26] K. Richter, R. Varga, G.A. Badini-Confolonieri, M. Vázquez, The effect of transverse field on fast domain wall dynamics in magnetic microwires, *Appl. Phys. Lett.* 96 (2010) 182507, <https://doi.org/10.1063/1.3428367>.
- [27] V. Zhukova, P. Corte-Leon, L. González-Legarreta, A. Talaat, J.M. Blanco, M. Ipatov, J. Olivera, A. Zhukov, Review of domain wall dynamics engineering in magnetic microwires, *Nanomaterials* 10 (2020) 2407, 291.
- [28] D. Atkinson, D.S. Eastwood, L.K. Bogart, Controlling domain wall pinning in planar nanowires by selecting domain wall type and its application in a memory concept, *Appl. Phys. Lett.* 92 (2008) 022510.
- [29] D.-Petit, A.-V. Jausovec, D. Read, R.P. Cowburn, Domain wall pinning and potential landscapes created by constrictions and protrusions in ferromagnetic nanowires, *J. Appl. Phys.* 103 (2008) 114307.
- [30] M. Ipatov, N.A. Usov, A. Zhukov, J. Gonzalez, Local nucleation fields of Fe-rich microwires and their dependence on applied stresses, *Physica B* 403 (2008) 379–381.
- [31] M. Vazquez, G.A. Basheed, G. Infante, R.P. Del Real, Trapping and injecting single domain walls in magnetic wire by local fields, *Phys. Rev. Lett.* 108 (2012) 037201.
- [32] P. Gawronski, V. Zhukova, A. Zhukov, J. Gonzalez, Manipulation of domain propagation dynamics with the magnetostatic interaction in a pair of Fe-rich amorphous microwires, *J. Appl. Phys.* 114 (2013) 043903.
- [33] V. Zhukova, J.M. Blanco, P. Corte-Leon, M. Ipatov, M. Churyukanova, S. Taskaev, A. Zhukov, Grading the magnetic anisotropy and engineering the domain wall dynamics in Fe-rich microwires by stress-annealing, *Acta Mater.* 155 (2018) 279–285.
- [34] P. Corte-León, V. Zhukova, J.M. Blanco, A. Chizhik, M. Ipatov, J. Gonzalez, A. Fert, A. Alonso, A. Zhukov, Engineering of domain wall propagation in magnetic microwires with graded magnetic anisotropy, *Appl. Mater. Today* 26 (2022) 101263, <https://doi.org/10.1016/j.apmt.2021.101263>.
- [35] D.-X. Chen, J.A. Brug, R.B. Goldfarb, Demagnetizing factors for cylinders, *IEEE Trans. Magn.* 27 (4) (1991) 3601–3619, <https://doi.org/10.1109/20.102932>.
- [36] A.P. Zhukov, M. Vázquez, J. Velázquez, H. Chiriac, V. Larin, The remagnetization process of thin and ultrathin Fe-rich amorphous wires, *J. Magn. Magn Mater.* 151 (1995) 132–138.
- [37] M. Ipatov, V. Zhukova, A.K. Zvezdin, A. Zhukov, Mechanisms of the ultrafast magnetization switching in bistable amorphous microwires, *J. Appl. Phys.* 106 (2009) 103902.
- [38] L. Gonzalez-Legarreta, P. Corte-Leon, V. Zhukova, M. Ipatov, J.M. Blanco, J. Gonzalez, A. Zhukov, Optimization of magnetic properties and GMI effect of thin Co-rich microwires for GMI microsensors, *Sensors* 20 (2020) 1588, <https://doi.org/10.3390/s20061588>.
- [39] Yu Kabanov, A. Zhukov, V. Zhukova, J. Gonzalez, Magnetic domain structure of microwires studied by using the magneto-optical indicator film method, *Appl. Phys. Lett.* 87 (2005) 142507.
- [40] J.N. Nderu, M. Takajo, J. Yamasaki, F.B. Humphrey, Effect of stress on magnetization process and the bamboo domains of CoSiB amorphous wires, *IEEE Trans. Magn.* 34 (1998) 1312–1314.
- [41] O.I. Akseonov, A.S. Aronin, Investigation of the domain structure of Co-based microwires by magneto-optical indicator films method, *Phys. Solid State* 63 (4) (2021) 513–518.
- [42] N.N. Orlova, A.S. Aronin, S.I. Bozhko, Yu P. Kabanov, V.S. Gornakov, Magnetic structure and magnetization process of the glass-coated Fe based amorphous microwire, *J. Appl. Phys.* 111 (2012) 073906, <https://doi.org/10.1063/1.3702448>.
- [43] N.N. Orlova, V.S. Gornakov, A.S. Aronin, Role of internal stresses in the formation of magnetic structure and magnetic properties of iron-based glass coated microwires, *Appl. Phys.* 121 (2017) 205108.
- [44] N.A. Buznikov, V.V. Popov, A core-shell model for magnetoimpedance in stress-annealed Fe-rich amorphous microwires, *J. Supercond. Nov. Magnetism* 34 (2021) 169–177.
- [45] V. Rodionova, M. Ipatov, M. Ilyn, V. Zhukova, N. Perov, J. Gonzalez, A. Zhukov, Tailoring of magnetic properties of magnetostatically-coupled glass-covered magnetic microwires, *J. Supercond. Nov. Magnetism* 24 (1–2) (2011) 541–547, <https://doi.org/10.1007/s10948-010-0989-0>.
- [46] V. Zhukova, J.M. Blanco, V. Rodionova, M. Ipatov, A. Zhukov, Fast magnetization switching in Fe-rich amorphous microwires: effect of magnetoelastic anisotropy and role of defects, *J. Alloys Compd.* 586 (2014) 287–290.
- [47] P. Corte-León, J.M. Blanco, V. Zhukova, M. Ipatov, J. Gonzalez, M. Churyukanova, S. Taskaev, A. Zhukov, Engineering of magnetic softness and domain wall dynamics of Fe-rich amorphous microwires by stress-induced magnetic anisotropy, *Sci. Rep.* 9 (2019) 12427, <https://doi.org/10.1038/s41598-019-48755-4>.
- [48] L. Kraus, L. The demagnetization tensor of a cylinder, *Czech. J. Phys.* 23 (1973) 512–519, <https://doi.org/10.1007/BF01593828>.
- [49] S. Gudoshnikov, N. Usov, A. Zhukov, J. Gonzalez, P. Palvanov, Measurements of stray magnetic fields of amorphous microwires using scanning microscope based on superconducting quantum interference device, *J. Magn. Magn Mater.* 316 (2007) 188–191.
- [50] G. Danilov, Yu Grebenschchikov, V. Odintsov, M. Churyukanova, S. Gudoshnikov, Measurements of stray magnetic fields of Fe-rich amorphous microwires using a scanning GMI magnetometer, *Metals* 13 (2023) 800, <https://doi.org/10.3390/met13040800>.
- [51] J. Stöhr, H.C. Siegman, *Magnetism, from Fundamentals to Nanoscale Dynamics*, Springer-Verlag Berlin Heidelberg, 2006, p. 822.
- [52] A. Zhukov, J.M. Blanco, A. Chizhik, M. Ipatov, V. Rodionova, V. Zhukova, Manipulation of domain wall dynamics in amorphous microwires through domain wall collision, *J. Appl. Phys.* 114 (2013) 043910, <https://doi.org/10.1063/1.4816560>.
- [53] S.A. Gudoshnikov, Yu B. Grebenschchikov, B. Ya Ljubimov, P.S. Palvanov, N. A. Usov, M. Ipatov, A. Zhukov, J. Gonzalez, Ground state magnetization distribution and characteristic width of head to head domain wall in Fe-rich amorphous microwire, *Phys. Stat. Sol. A* 206 (4) (2009) 613–617, 2009.
- [54] F. Beck, J.N. Rigue, M. Carara, The profile of the domain walls in amorphous glass-covered microwires, *J. Magn. Magn Mater.* 435 (2017) 21–25.
- [55] M. Kládiová, J. Ziman, Properties of a domain wall in a bi-stable magnetic microwire, *J. Magn. Magn Mater.* 480 (2019) 193–198.
- [56] M. Kládiová, J. Ziman, Contribution to the study of the domain wall shape in bistable microwires, *J. Magn. Magn Mater.* 537 (2021) 168108.
- [57] O. Vahovsky, R. Varga, K. Richter, Experimental method for surface domain wall shape studies in thin magnetic cylinder, *J. Magn. Magn Mater.* 483 (2019) 266–271.
- [58] L.V. Panina, M. Ipatov, V. Zhukova, A. Zhukov, Domain wall propagation in Fe-rich amorphous microwires, *Physica B* 407 (2012) 1442–1445, <https://doi.org/10.1016/j.physb.2011.06.047>.
- [59] A. Chizhik, J. Gonzalez, A. Zhukov, P. Gawronski, M. Ipatov, P. Corte-León, J. M. Blanco, V. Zhukova, Reversible and non-reversible transformation of magnetic structure in amorphous microwires, *Nanomaterials* 10 (8) (2020) 1450.
- [60] D. Kumar, T. Jin, R. Sbiaa, M. Kläui, S. Bedanta, S. Fukami, D. Ravelosona, S.-H. Yang, X. Liu, S.N. Piramanayagam, Domain wall memory: physics, materials, and devices, *Phys. Rep.* 958 (2022) 1–35.
- [61] D. Atkinson, C.C. Faulkner, D.A. Allwood, R.P. Cowburn, Domain-wall dynamics in magnetic logic devices, in: B. Hillebrands, A. Thiaville (Eds.), *Spin Dynamics in Confined Magnetic Structures III*, Top, vol. 101, Appl. Phys., 2006, https://doi.org/10.1007/10938171_6.
- [62] R. Moriya, M. Hayashi, L. Thomas, C. Rettner, S.S.P. Parkin, Dependence of field driven domain wall velocity on cross-sectional area in $\text{Ni}_{65}\text{Fe}_{20}\text{Co}_{15}$ nanowires, *Appl. Phys. Lett.* 97 (2010) 142506, <https://doi.org/10.1063/1.3494521>.
- [63] Y. Tanaka, T. Hirai, T. Koyama, D. Chiba, Electric-field-induced magnetic domain writing in a Co wire, *APEX* 11 (2018) 053005, <https://doi.org/10.7567/APEX.11.053005>.
- [64] P. Ho, K.-H. Tu, J. Zhang, C. Sun, J. Chen, G. Lontos, K. Ntetsikas, A. Avgeropoulos, P.M. Voyles, C.A. Ross, Domain configurations in Co/Pd and L10-FePt nanowire arrays with perpendicular magnetic anisotropy, *Nanoscale* 8 (2016) 5358–5367.